AGU ADVANCING EARTH AND SPACE SCIENCES

Water Resources Research

RESEARCH ARTICLE

10.1029/2024WR038754

Undervalued Groundwater Resources Over the Major Tectonic Lines of Southeastern China

Michele Lancia[1,2], Lihong Yang[2,3,4], Zhijie Liu[4], Jianan Xu[1,5], Jiang Yu[1,2,3], Stefano Viaroli[6], Junfei Zou[4], Charles B. Andrews[7], and Chunmiao Zheng[1,2,3]

[1]Eastern Institute for Advanced Study, Eastern Institute of Technology, Ningbo, China, [2]State Environmental Protection Key Laboratory of Integrated Surface Water-Groundwater Pollution Control, School of Environmental Science and Engineering, Southern University of Science and Technology, Shenzhen, China, [3]Guangdong Provincial Key Laboratory of Soil and Groundwater Pollution Control, School of Environmental Science and Engineering, Southern University of Science and Technology, Shenzhen, China, [4]SUSTech Environmental Inc., Shenzhen, China, [5]School of Environmental Science & Engineering, Shanghai Jiao Tong University, Shanghai, China, [6]Department of Earth Sciences, University of Pisa, Pisa, Italy, [7]S.S. Papadopulos & Associates, Inc., Rockville, MD, USA

Key Points:

- Rural areas in southeastern China possess exploitable groundwater resources within fractured bedrock near major tectonic fault lines
- Field investigations and numerical modeling provide insights into the dynamics and potential exploitation of these fractured aquifers
- Mapped distributions reveal fractured basins with inferred groundwater resources throughout southeastern China

Supporting Information:

Supporting Information may be found in the online version of this article.

Correspondence to:

L. Yang and C. Zheng,
yanglh@sustech.edu.cn;
zhengcm@sustech.edu.cn

Citation:

Lancia, M., Yang, L., Liu, Z., Xu, J., Yu, J., Viaroli, S., et al. (2025). Undervalued groundwater resources over the major tectonic lines of southeastern China. *Water Resources Research*, *61*, e2024WR038754. https://doi.org/10.1029/2024WR038754

Received 26 AUG 2024
Accepted 12 FEB 2025

Author Contributions:

Conceptualization: Michele Lancia, Lihong Yang, Charles B. Andrews
Data curation: Michele Lancia, Jianan Xu, Jiang Yu
Formal analysis: Michele Lancia
Funding acquisition: Lihong Yang, Chunmiao Zheng
Investigation: Zhijie Liu, Jianan Xu, Stefano Viaroli, Junfei Zou
Methodology: Michele Lancia, Lihong Yang, Stefano Viaroli, Chunmiao Zheng
Project administration: Lihong Yang, Zhijie Liu

Abstract

Rising water demand for agricultural, industrial, and domestic sectors continue to stress water resources worldwide. In southeastern China, coastal cities and megacities typically rely on thousands of reservoirs, incurring high construction and maintenance costs. However, rural areas in this region, underlain by shallow, low-permeability bedrock due to regional metamorphism, host exploitable groundwater resources along major tectonic fault lines. To understand groundwater dynamics in these fractured aquifers, this study investigates a local site in Longquan (Zhejiang Province, China). Field investigations informed a three-dimensional geological model, which provided the basis for numerical flow modeling analysis using the USGS-MODFLOW code. Results indicate that permeable damage zones along the tectonic fault lines are recharged by a weathered bedrock blanket layer and are laterally bounded by low-permeability bedrock, limiting the spatial extension of the aquifer. The sub-tropical climate and hydrostratigraphic conditions make groundwater exploitation feasible, despite the modest groundwater yield of the damage zones (2.2×10^5 m^3 per km of damage zone). Intensified fracturing also produces recognizable morphological changes, transitioning from steep, incised valleys to rounded hills with flatter streambeds. This distinctive morphological feature was identified in 140 basins across southeastern China, suggesting the presence of strategic groundwater resources throughout this region. Harnessing these fracture-controlled groundwater resources may bolster economic growth in rural communities and help narrow the development gap with more urbanized coastal areas.

Plain Language Summary

Southeastern China satisfies the water demand of cities and megacities with thousands of reservoirs that collect abundant rainfall. The water distribution disfavors rural areas, often located far from the water infrastructures. Fractured aquifers are present along major fault zones due to the intense tectonic activity that affected these areas over geological time. The characterization of a fractured basin in Longquan (Zhejiang, China) was conducted to understand the dynamics of this aquifer type, with scenarios encompassing water abstraction from water wells under normal and prolonged drought conditions. Other potential sites with similar characteristics were mapped throughout southeastern China. Inexpensive geophysical exploration can locally verify the occurrence of these fractured aquifers. The groundwater exploitation of these basins can promote the economic growth of the internal rural areas, reducing the gap with the coastal urban areas of southeastern China.

1. Introduction

Climate variability and urbanization have stressed water resources worldwide, with the depletion of surface water and groundwater resources (Rodell et al., 2018). In the last decades, the construction of water reservoirs has supplied an increment of freshwater storage to support increasing water demand, mitigate flood risk, and support the global generation of electricity with hydropower schemes (Lehner et al., 2011). Despite their unquestionable strategic value, water reservoirs require high costs for construction and maintenance and progressively trap the sediments of the inflowing rivers and streams, with a decrement in the water storage over time (Wu et al., 2022). Water reservoirs also impact wildlife and favor coastline erosion due to the reduction of sediment input (Brandt, 2000).

Resources: Lihong Yang, Zhijie Liu, Junfei Zou
Software: Michele Lancia, Jiang Yu, Chunmiao Zheng
Supervision: Lihong Yang, Charles B. Andrews, Chunmiao Zheng
Validation: Michele Lancia, Jiang Yu
Visualization: Michele Lancia, Jiang Yu
Writing – original draft: Michele Lancia
Writing – review & editing: Lihong Yang, Charles B. Andrews, Chunmiao Zheng

On the contrary, groundwater exploitation in favorable hydrogeological conditions requires limited infrastructures as the distance between the water wells and users is easier to optimize. In addition, groundwater resources are not as affected by seasonal climate extremes as hydrogeological variations generally occur on a longer temporal scale (Kuang et al., 2024). Because of the appeal and economic convenience of groundwater exploitation, many groundwater systems worldwide have been seriously depleted (Jasechko et al., 2024). Groundwater overexploitation throughout alluvial plains and coastal areas has led to large piezometric cones of depression in many agricultural and industrialized areas, together with groundwater pollution, subsidence, and saline intrusion (Famiglietti, 2014).

The Chinese transition from a developing country to a world factory (Zhang, 2006) has depleted the water resources, with a groundwater loss of about 17 $km^3\ y^{-1}$ in the last 75 years (Lancia et al., 2022). In China (Figure 1a), there is a dichotomy between the dry northern plains, relying on stressed groundwater resources, and southern hilly terrain with abundant rainfall collected by thousands of water reservoirs (Zheng et al., 2010). China has 22,000 large dams with a total water storage capacity of 510 km^3 (Tigrek & Aras, 2011) with an estimated storage loss due to sediment trapping equal to 12 $km^3\ y^{-1}$ (White, 2001). The successful South-to-North Water Transfer project, aiming at transferring a water volume of 45 $km^3\ y^{-1}$ when completed (Long et al., 2020), satisfies the total Chinese water balance but increases the dependency of Chinese water demand on surface water resources.

The Chinese economic transition has favored the development of large urban areas deepening the gap with rural areas, causing large socioeconomic disparity, and harming long-term economic growth (Yao & Jiang, 2021). Incremental improvements in living standards (United Nations, 2023) in rural areas and new policies, such as the introduction of sanitary toilets nationwide (Cheng et al., 2024), have partially mitigated the gap with the urban areas at the expense of increased water demand.

In southeastern China (Figure 1b), surface water satisfies 97% of the total water demand, about 33 $km^3\ y^{-1}$ (Shen, 2021). The remaining 3% of the water demand is met mainly by groundwater extraction from stressed urban unconsolidated aquifers. This extraction occurs primarily along the coastline and has resulted in diffuse saline intrusions and groundwater quality degradation (Fu et al., 2022). Mountainous and hilly sectors of southeastern China have large but undervalued groundwater resources, about 60 $km^3\ y^{-1}$ (Shen, 2021), concentrated in the shallow aquifers of the weathered bedrock. This groundwater resource has been sparsely exploited because of limited knowledge of fractured zones and their potential to yield substantial groundwater as the bedrock in general has low yield and storativity (Lancia et al., 2022).

However, the damage zones associated with the major and minor tectonic fault lines are often fractured aquifers that can locally store important groundwater resources (Scibek, 2020). Tectonic processes have caused fracture propagation within the bedrock media, locally increasing the hydraulic conductivity and storativity (Bense et al., 2013), and also favoring the rise of hot fluids with economic opportunities for possible geothermal exploitations (Medici et al., 2023). The groundwater exploitation of the damage zone is challenging as hydraulic properties along the fault zones are typically heterogeneous due to the occurrence of ductile shear zones (Liu et al., 2017).

Because of the hilly and mountainous morphology, these inland areas are difficult to serve with regional water infrastructure. The use of groundwater resources could avoid the construction of small water reservoirs, saving the energy costs to transport the water to villages located at different elevations, the expenses of dam construction and maintenance, as well as ecosystems preservation. Thus, despite the geological difficulties, the exploitation of these undervalued groundwater resources is strategic for the rural areas of southeastern China.

The groundwater dynamics of these damage zones was investigated at the local scale at a site in Longquan (Zhejiang, China), characterized by extensive field investigations and numerical analyses (Figure 1c). Groundwater pumping scenarios during drought are simulated to evaluate the response of these groundwater systems to climate stress. Based on the evidence from the Longquan site, criteria to identify fractured aquifers at other sites of southeastern China are proposed.

The objectives of this research were to: (a) quantify the groundwater resources of the local basin based on extensive field surveys and numerical models; (b) evaluate the response of these groundwater systems to climate stress; and (c) identify similar fractured basins throughout southeastern China using morphological criteria.

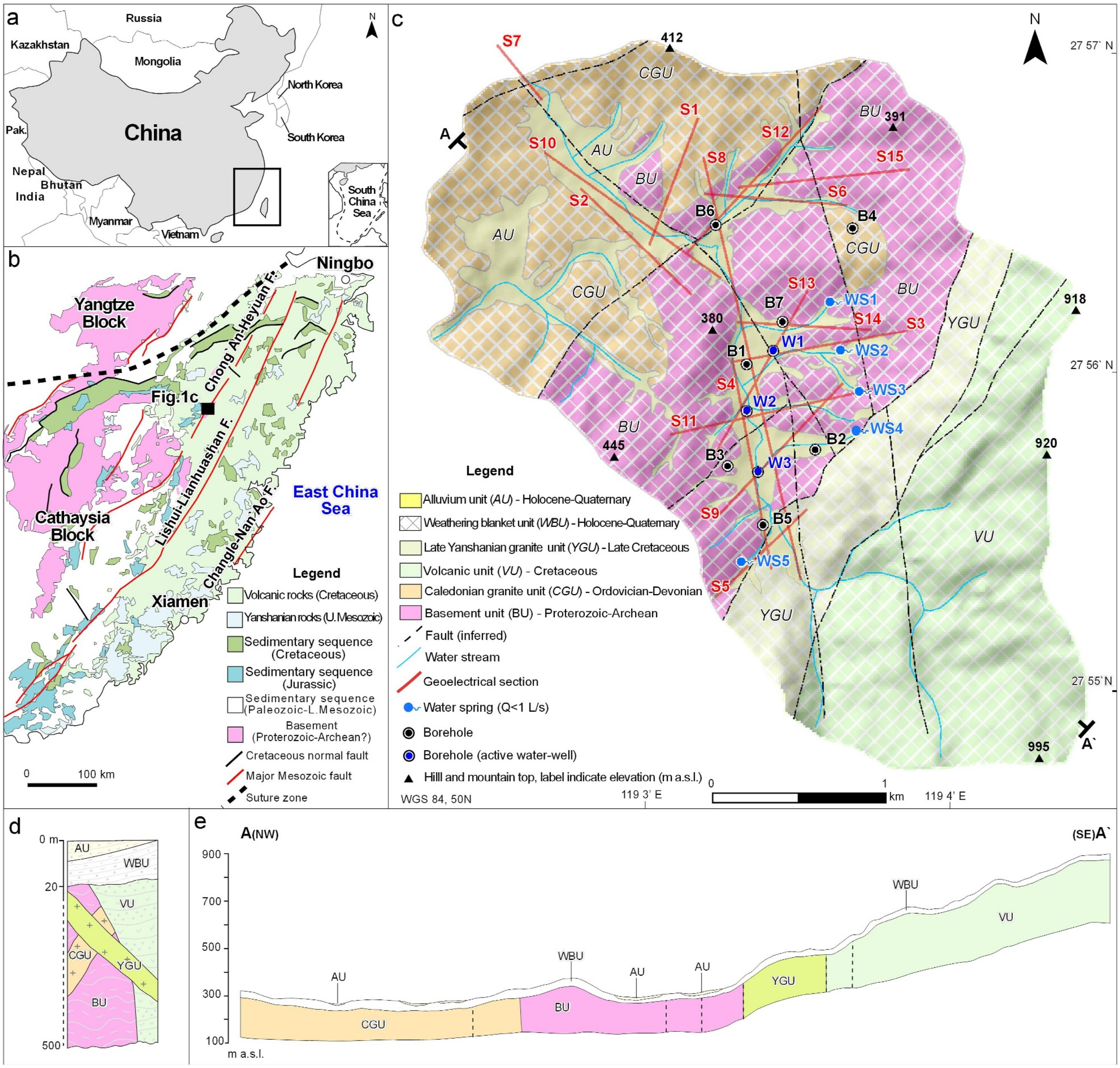

Figure 1. (a) China map, the black box indicates southeastern China, (b) simplified tectonic scheme of southeastern China, redrawn from Li et al. (2014), (c) hydrogeological map of Longquan site, (d) with stratigraphic column, and (e) cross-section A-A'.

2. Materials and Methods

2.1. Hydrogeological Background

Southeastern China (Figure 1b) has a subtropical climate, with an average annual rainfall between 1,300 to 2,000 mm y^{-1}. The morphological relief is alternated with narrow alluvial valleys that are the result of a complex geological evolution encompassing Mesozoic contractional and extensional tectonics on preexisting North-northeast to South-southwest (NNE-SSW) lines (Wan, 2010). The major tectonic lines with a regional extension are the Chong'An-Heyuan fault, the Lishui-Lianhuashan fault, and the Changle-Nan`Ao fault (Figure 1b). The tectonic disruption of the pre-Mesozoic basement favored the intrusion of granitic rocks and volcanic masses that currently constitute the major relief in the area. The narrow valleys, with thin Quaternary sequences, are developed along the NNE-SSW trend, illustrating the strong control of tectonics on watershed morphology.

At the regional scale, the bedrock sequences have low hydraulic conductivity due to the occurrence of regional metamorphism that reduced the aperture of the fractures (Campbell & Sewell, 1997). Groundwater flow is concentrated in the weathered blanket (i.e., laterite soils) of the bedrock units that serve as a shallow aquifer. The weathered blanket sustains the baseflow of mountain streams and laterally recharges the coarse layers of the alluvial valleys (Lachassagne et al., 2014; Lancia et al., 2020). At the local scale, the damage zones produced by the major tectonic lines, arranged parallel to the fault planes, increase the aquifer storage of the bedrock. The groundwater potential of these fractured aquifers and their occurrence over the major tectonic lines were investigated at the Longquan site (Figure 1c).

2.2. The Longquan Site

The Longquan site (~9.5 km^2) is a small agricultural center producing rice, tea, and canola with an average precipitation of ~1,700 mm y^{-1} (Figure S1a in Supporting Information S1). An alluvial valley connects several small and elongated tectonic basins (Figure 1c), located along the Chong'An-Heyuan fault (Figure 1b). The highest areas, reaching ~1,000 m a.s.l., are located at the southeastern edge and are incised by streams that follow the North-northwest to South-southeast and NNE-SSW trends (Figure 1c). Pre-existing geophysical surveys for the construction of water infrastructure noted developed bedrock fractures throughout the basin. Subsequent field surveys, borehole drilling, and pumping tests highlighted exploitable groundwater resources. From a hydrogeological point of view, the geologic sequences of the Longquan site can be simplified into six units (Figure 1d).

- The alluvial unit (AU) occupies the bottom of the alluvial valleys and consists of clayey sands alternated with quartz sands. The facies alternation is a response to the tectonic and climatic variations that have sorted the sediment. The unit is a local aquifer with a thickness from 5 to 10 m (Quaternary-Holocene)
- The weathered blanket unit (WBU) is ubiquitous in the catchment. As depth increases, layers of reddish clayey sands transition into quartz sands and breccia. The unit represents a consistent shallow aquifer feeding springs and mountain streams (Figure 1c). The unit thickness varies between 20 and 40 m from ground level (Quaternary - Holocene)
- The Yanshanian granite unit (YGU) is located at the piedmont of the southeastern slope. The unit outcrops in a small narrow band tectonically placed between volcanic unit (VU) and basement unit (BU). The limited number of outcrops show a competent bedrock without open fractures, suggesting they function as an aquitard (Late Cretaceous)
- The VU includes several lava flows and tuffs with a low primary porosity. The unit constitutes the major relief in the southwestern sector (Figure 1c). The bedrock outcrops have sparse fractures, suggesting they also function as an aquitard (Cretaceous)
- The Caledonian granite unit (CGU) has characteristics similar to the YGU (Ordovician - Devonian)
- The BU is an alternation of metagranulites, quartz schists, and mica schists. The bedrock outcrops are characterized by numerous fractures filled with quartz veins conferring the unit with aquitard properties (Archean? - Proterozoic?)
- Inner fault (FI) and outer fault (FO) damage zones are found in the borehole logs and consist of saturated layers of breccia, sand, and silt alternated with fractured bedrock.

2.2.1. Field Investigations

The lush subtropical vegetation together with the weathering blanket unit masks the bedrock outcrops. Information on the fracturing is limited, as bedrock fracturing can only be observed along fresh road cuts and streams. Fault planes are masked by the dense vegetation and data about tectonic kinematics cannot be retrieved from field surveys. Even recent excavations rapidly weather and are covered by vegetation and are of limited use for geological analyses. Thus, in the absence of kinematic information on faults, the mapped tectonic contacts among the different units are assumed sub-vertical. Field surveys have mapped five springs that originate at the contact between WBU and BU (Figure 1c), providing information on the water-table elevation along the slope.

To better understand the geometry of the damage zones, 15 geoelectrical sections were carried out throughout the basin. The locations of the sections were optimized to not impact the activities of the local population and to avoid possible electrical interference with the urban infrastructure. Each section consisted of numerous electrodes, variable between 80 and 200, connected to a DUK-4 resistivity/Induced Polarization surveying system (China Geological Instruments, Chongqing). The data were processed using the RImager software developed by Geogiga

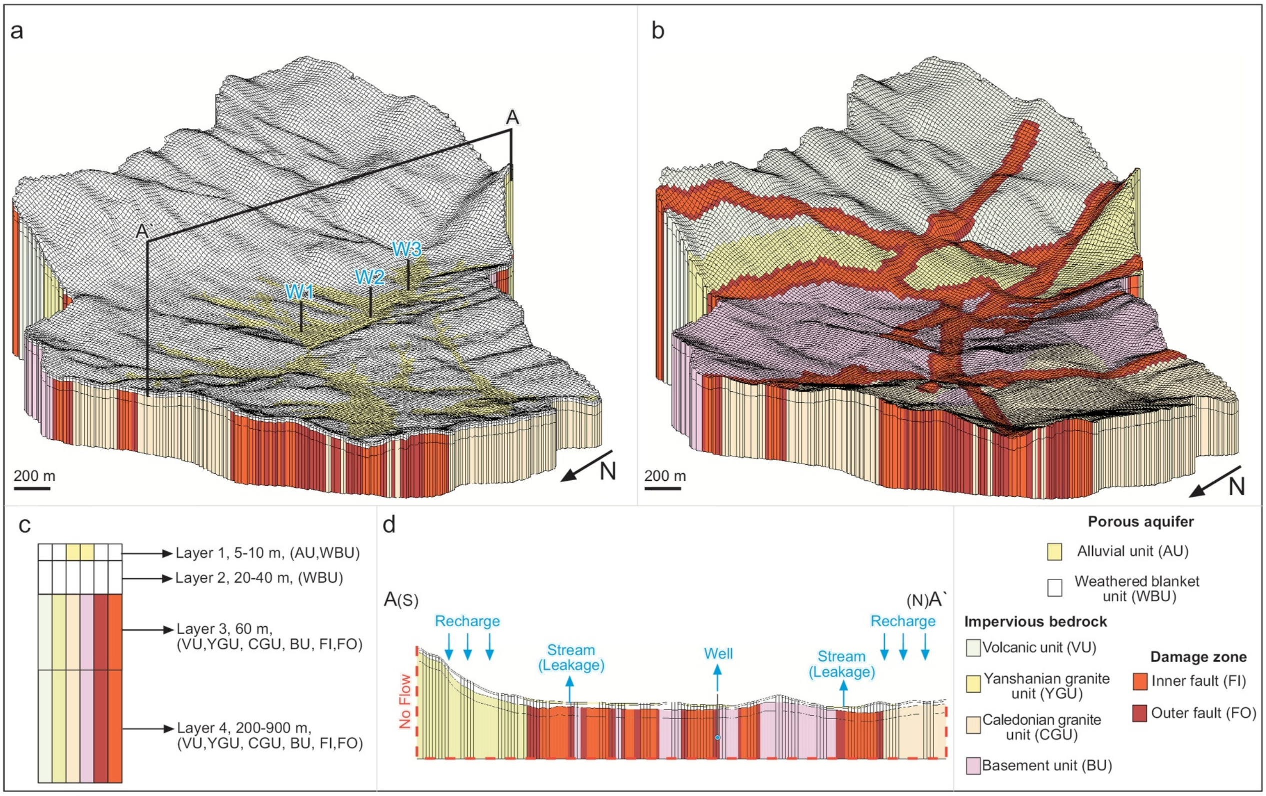

Figure 2. (a) MODFLOW three-dimensional grid, (b) MODFLOW three-dimensional grid with the first and second layer inactivated to highlight the distribution of the aquitard bedrock and the damage zones, (c) summary vertical column synthesizing the distribution of the units and their thickness, (d) numerical section with boundary conditions.

Technology Corporation (Calgary, Canada). Each section was interpreted to trace the limit between WBU and the other bedrock units as well as to trace the major tectonic elements of the site (Figure S2a in Supporting Information S1).

The advancement of 10 boreholes provided a direct characterization of the bedrock and associated damage zones. Among these boreholes, the three most productive were transformed into water wells for mineral water production, with working flow rates of ~6 L s^{-1}. According to the preliminary geophysical investigations, boreholes were concentrated in the BU and CGU, which is locally more fractured and offers a higher probability of exploitable groundwater resources. The depth below ground surface of the boreholes varied between 150 and 170 m. The borehole logs confirmed the presence of AU and the WBU in the first 20–40 m. The three water wells were further investigated with simultaneous pumping tests (recovery step test) with a total duration of ~24 days.

2.2.2. Three-Dimensional Model

Data from field surveys, geophysical investigations, and borehole logs were merged to build a three-dimensional geological model of the Longquan site (Figure S2b in Supporting Information S1). The digital elevation model (DEM) ALOS-PALSAR with a resolution of 12.5 m was imported into Groundwater Modeling System (GMS) Aquaveo. The hydrogeological map (Figure 1c) was projected on the DEM surface as a triangular irregular network. The fault planes (Figure S2c in Supporting Information S1) were reconstructed via the cross-correlation of geological sections and data from field surveys. Due to the limited available information, the following assumptions guaranteed a simplified construction of the three-dimensional model for groundwater purposes: (a) inferred faults and contact among bedrock units (Figure 2d) were assumed sub-vertical; (b) the weathered blanket was assumed to be 30 m thick, parallel to the topography (Figure S2e in Supporting Information S1); and (c) bedrock units were schematized as terrain blocks delimited at the bottom by flat surfaces at 500 m below sea level. The constructed geologic model was converted into a MODFLOW grid to simplify numerical analyses.

2.3. Numerical Setup

The model domain was discretized via four layers and a square grid 20 m on a side (Figure 2a). The first two layers represent the AU and WBU while the third and fourth layers represent the aquitards (VU, YGU, CGU, and BU) and the damage zone units (Figure 2b). The thickness of the first layer varies from 5 to 10 m and was optimized to represent the lateral transition between the AU and the WBU (Figure 2c). The second layer was introduced to increase the thickness of WBU up to 40 m from the ground surface. The third and fourth layers represent the lateral heterogeneities of the aquitard bedrock (VU, YGU, CGU, and BU). In correspondence with the faults, the damage zones were delineated. These features were subdivided into an internal damage zone (FI), ~100 m wide, delimited by two external damage zones (FO), ~20 m wide (Figure 2c).

The model uses the Newton formulation in combination with the unsaturated zone flow which provides good convergence for unconfined aquifers distributed along a mountain morphology as all cells are kept active during the simulation (Harbaugh, 2005; Niswonger et al., 2011). On the highest active cell, calibrated aquifer recharge was simulated (Figure 2d). If the simulated water table was higher than the elevation of the first layer, recharge was reduced and groundwater to surface water flow was accounted for as leakage (Figure 2d). The Well package was used to simulate the water abstraction from the active water wells, specified in the fourth layer. No-flow boundaries were applied at the edges and the bottom of the domain (Figure 2d). This assumption is valid for the steady-state simulations, without groundwater pumping, as the groundwater basin mostly coincides with the hydrologic watershed. During the simulations, this simplification was tested in transient conditions, verifying that simulated drawdowns, representing the effects of groundwater pumping on hydraulic head distribution, were negligible on the boundaries of the model domain.

Two transient models were built. The first transient model simulated the pumping tests performed in the field (schematized in Figure S3 in Supporting Information S1). In this transient simulation, time was discretized with three stress periods with 50 time steps each. Each stress period coincides with the duration of the pumping test step performed on the field. An initial steady-state stress period was used to calculate initial conditions for the transient simulation.

After the calibration in transient conditions, the second transient model was built to assess the long-term effects of pumping from the three active water wells, with a pumping rate of 6 L s^{-1}, for 5 years. Time was discretized into 61 stress periods (duration 1 month), and each stress period had five-time steps. In this long-term analysis, the average calibrated recharge rate was obtained by multiplying the average monthly rainfall by the annual percentage recharge to simulate the seasonal wet and dry periods (Figure S1b in Supporting Information S1). At the end of the five years, an additional stress period (6 months duration with 12-time steps) with a null recharge was used to simulate a severe drought scenario.

3. Results

3.1. Calibration and Parametrization

Model calibration was achieved via a two-step analysis that combined steady-state and transient observations (Figure S3a in Supporting Information S1). First, a preliminary steady-state model, without groundwater pumping from water wells, was calibrated via a manual trial-and-error approach. Calibration was performed with average water levels of springs and water wells, focusing on recharge parameters (Figure S3b in Supporting Information S1). The initial value range for calibration of recharge was 15%–30% of the average annual precipitation (annual percentage recharge). In the second step of the analysis, hydraulic conductivity and storativity were calibrated using a second transient model obtained from a simultaneous pumping test of the three active water wells (Figure in Supporting Information S1). The calibrated solution in steady-state conditions was used as the starting head solution. Initial hydraulic conductivity and storativity values of rocks and soils were estimated from the literature (Freeze & Cherry, 1979). To match the observed and the simulated pumping test drawdowns, point observations were extrapolated from the available plots of drawdown during the pumping tests. The Parameter Estimation algorithm implemented in GMS Aquaveo was used to assist in the calibration (Doherty, 2021). The entire calibration process was repeated three times to achieve the best calibration for transient conditions (Figure S3a in Supporting Information S1). The values of the hydraulic parameters are listed in Table 1.

The conceptual model and the calibrated parameters are consistent with field observations. The WBU and the AU constitute a continuous shallow aquifer with a hydraulic conductivity equivalent to a silty sand (Freeze &

Table 1
Hydraulic Parameters of the Longquan Site

	Rch [mm y^{-1}]	$\frac{Rch}{Rainfall}$ [%]	k [m s^{-1}]	Storativity Sy	Storativity Ss [m^{-1}]
Unit					
Alluvial Unit (AU)	60	3.5	5 10^{-5}	0.1	(-)
Weathered Blanket Unit (WBU)	440	23.5	1 10^{-6}	0.1(Layer 1)	
				0.3 (Layer 2)	
Yanshanian Granite Unit (YGU)	(-)	(-)	1 10^{-9}	0.001	1 10^{-8}
Volcanic Unit (VU)		(-)	1 10^{-9}	0.001	1 10^{-8}
Caledonian Granite Unit (CGU)		(-)	1 10^{-9}	0.001	1 10^{-8}
Basement Unit (BU)		(-)	5 10^{-9}	0.001	1 10^{-8}
Damage zone					
Inner Fault (FI)	(-)	(-)	2.5 10^{-5} (Layer 3)	0.01	1 10^{-8}
		(-)	4 10^{-6} (Layer 4)		
Outer Fault (FO)		(-)	6 10^{-5} (Layer 3)	0.01	1 10^{-8}
		(-)	1 10^{-6} (Layer 4)		

Note. Rch is the average annual recharge, *k* is the hydraulic conductivity, Sy is the specific yield, and Ss is the specific storage (-) indicates no value.

Cherry, 1979). Similar hydraulic conductivity values for the AU and WBU are consistent as the alluvial deposits are derived from the laterite soils of the weathered blanket. The reduced simulated recharge rate of the AU is likely due to the occurrence of rice paddies that have resulted in the locally accumulation of finer soils at the surface over time. The increment of specific yield between the first and the second layers of WBU is related to the occurrence of sand and breccia layers in contact with the bedrock unit.

The calibrated dataset is also consistent with the intact bedrock units functioning as aquitards, with negligible groundwater storage. The damage zones (FI and FO) are local aquifers with hydraulic conductivity ranges comparable with the AU and WBU. The decreased hydraulic conductivity between the third and fourth layers is related to fracture aperture reduction with depth due to increasing lithostatic load. The higher hydraulic conductivity value of the FO, compared to FI, is reasonable based on the occurrence of metamorphosed rocks at the fault core that locally reduces the hydraulic conductivity (Caine et al., 1996). The specific yield of FI and FO, about one order of magnitude lower than AU and WBU, is reasonable as the damage zones include layers of bedrock with reduced specific yield. The hydraulic heterogeneities of the damage zones were confirmed by interpreting the occurrence of a hydraulic barrier, from the spatial distribution of drawdown generated during the pumping test of W1 (Figure S3c in Supporting Information S1).

3.2. Groundwater Dynamics and Flow Budgets

The model simulates groundwater flow from the areas of high relief to the valleys, controlled by the geological characteristics of the subsoils. The simulated groundwater heads among the four layers are slightly different due to the vertical components of groundwater flow. The water table occurs in the bedrock in the higher relief areas and within the unconsolidated layers near the basin. This is typical of mountain catchments with large morphological variations and thin shallow aquifers.

The fourth layer, with the simulated water wells, is of particular interest for groundwater management purposes (Figure 3a). In the southeastern sector of the basin, the water table has a strong gradient that rapidly dissipates as the water table intersects the damage zone located along the piedmont (Figure 3b). Damage zones create a preferential direction of groundwater flow, locally influencing the piezometric field.

The simulated cones of depressions triggered by groundwater pumping developed rapidly in early time and then remained steady for the next 5 years of the simulations (Figure 3c). Simulated drawdown patterns are asymmetrical, and their spatial development is affected by the vertical heterogeneities of the subsoil. After 5 years of

10.1029/2024WR038754

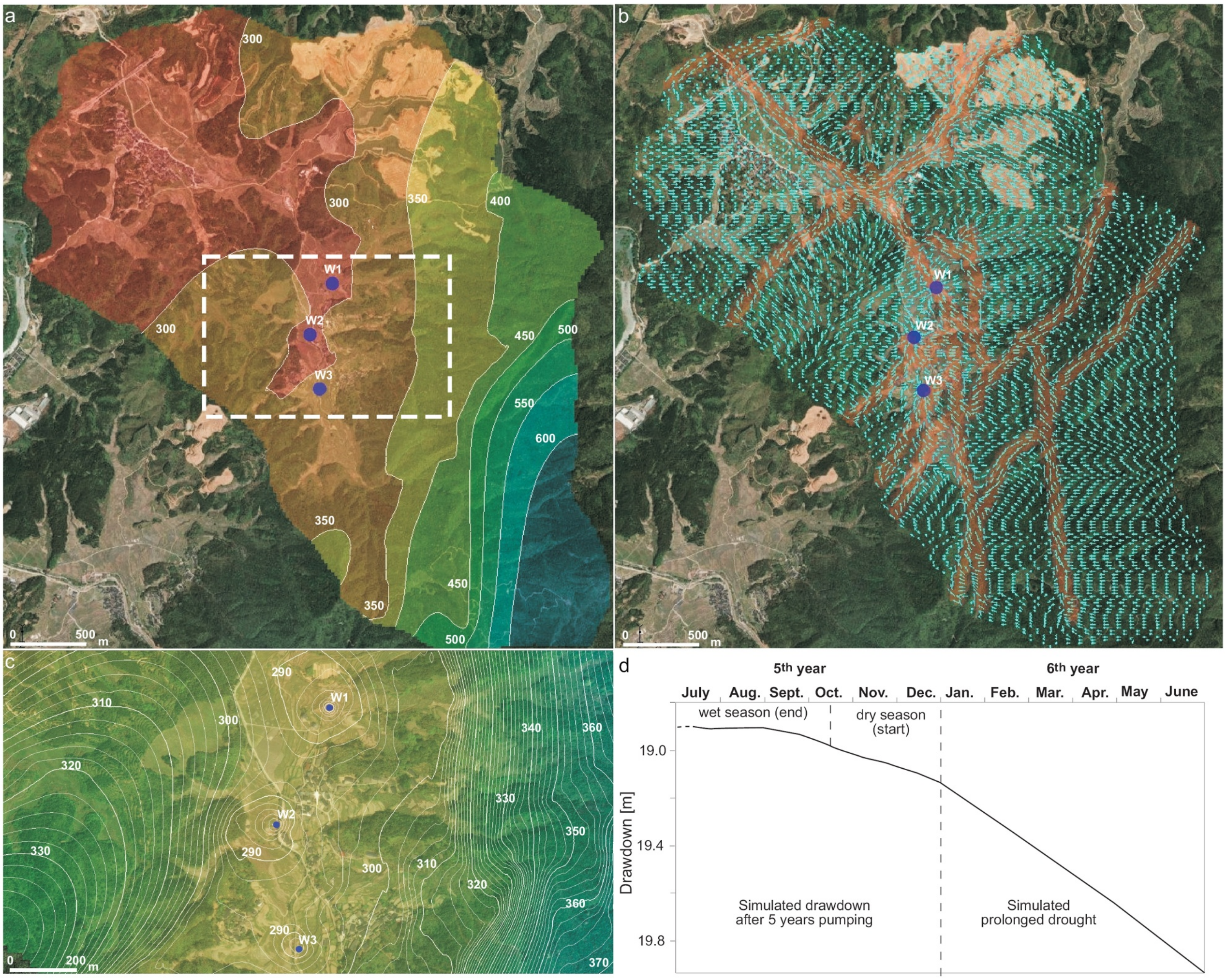

Figure 3. (a) Groundwater head map, (b) groundwater flow vectors (cyan arrows), and damage zones (tan bands), (c) groundwater head close-up (white dashed box) with the cone of depressions developed after 5 years of simulated pumping, and (d) simulated drawdown (average among W1, W2, and W3 water wells) after 5 years of pumping and 6 months of drought with zero aquifer recharge.

simulated groundwater pumping, the damage zones at the edge of the domain have negligible drawdown confirming that the no-flow boundary conditions at the edge of the model are appropriate for the simulated pumping rate.

The simulation of a severe drought of 6 months, with the recharge specified as zero, was also simulated (Figure 3d). The average water table variation of the three water wells is plotted (Figure 3d). Average drawdown slowly decreased from 19.1 to 19.9 m in 6 months, demonstrating that the simulated aquifer has a sustainable yield under drought conditions.

4. Discussions

4.1. Groundwater Pumping Sustainability

The model simulates groundwater pumping from damage zones along major tectonic features characterized by limited storage. As the bedrock has low hydraulic conductivity and damage zones have a limited storativity, groundwater pumping is sustained by the shallow aquifers (AU and WBU) that replenish the damage zones via vertical leakage (Figure 4). The total yield of the damage zone is estimated as 2.2 10^5 m^3 per km of damage zone while the total yield of the saturated shallow aquifer (AU and WBU) is about 7 10^6 m^3 per km^2. The continuous

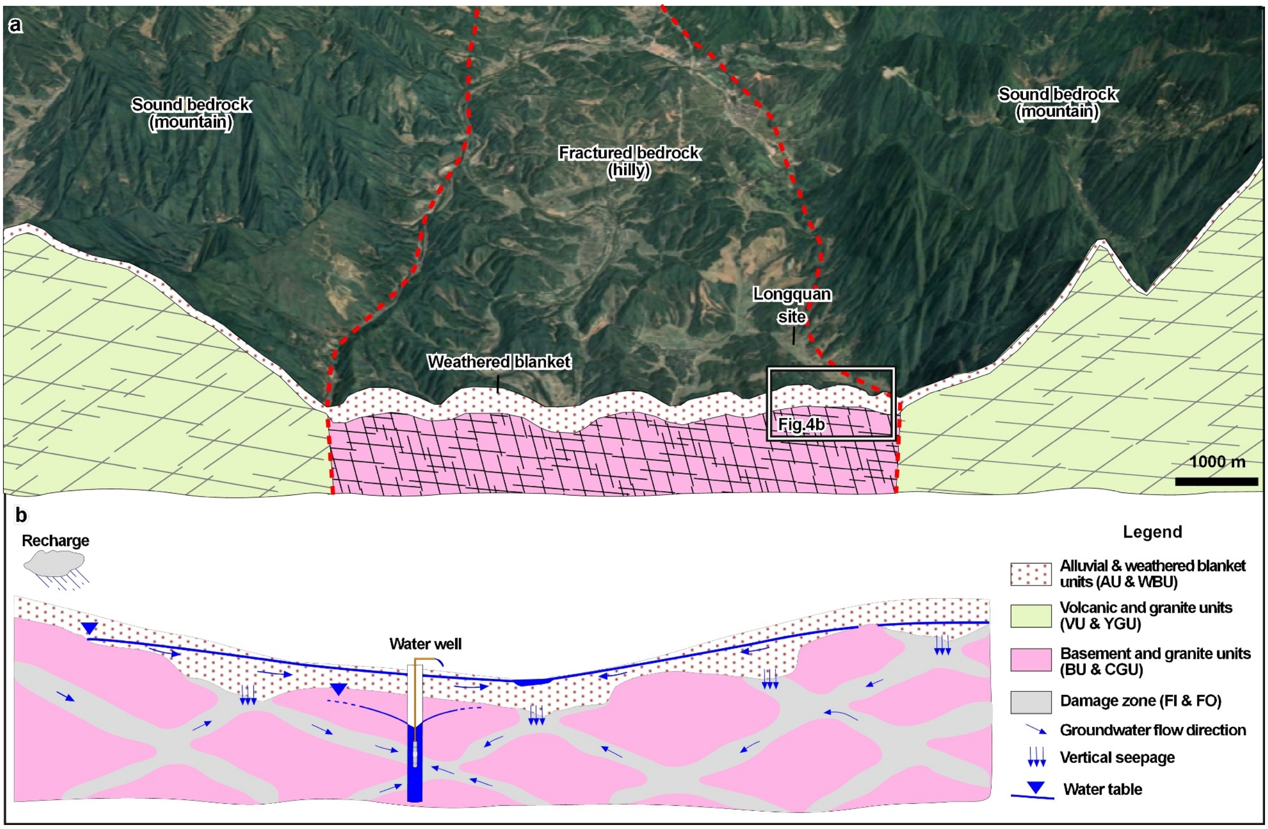

Figure 4. (a) Groundwater conceptual model of the Longquan site (vertical exaggeration 3×), the red lines indicate the transition from a mountain to hilly morphology associated with an increase of the fracture density, and (b) the shallow aquifer units (alluvial unit and weathered blanket unit) discharge to streams and recharge the damage zones (Inner fault and outer fault), via vertical leakage when water wells are present.

groundwater pumping triggers a reduction in the groundwater discharge to surface streams, reducing their baseflows.

In the transient simulations, some of the water that recharges the aquifer flows laterally and sustains the baseflow of mountain streams, and some flows vertically toward deep fractured aquifers that sustain the water abstraction of water wells (Figure 4). The modest hydraulic conductivity of the shallow aquifers reduces the groundwater to surface water exchange, favoring the vertical seepage flow. Stored groundwater remains available to sustain the water pumping during a prolonged drought. However, during the 6 months of simulated drought, the groundwater discharge to surface water was reduced by 27% (from 84 to 61 L s^{-1}). Groundwater abstraction has impacts on shallow water resources, as shallow water and aquifer damage zones are interconnected via the weathered blanket aquifers. Even when damped by the weathered blanket aquifer, over pumping from the damage zones may lead to streams drying up with associated ecological damage.

The groundwater schemes in these contexts have numerous hydrological advantages compared to shallow groundwater exploitation, despite the numerous limitations of the evaluations. Deep groundwater resources are less vulnerable than shallow groundwater resources to agricultural contaminants. In addition, the construction of small artificial reservoirs to capture surface-water runoff would locally significantly increase water evaporation at these latitudes.

Despite the numerous hydrological advantages, a potential downside of the groundwater exploitation of these fractured aquifers is water quality. The impoverishment of the groundwater quality can be triggered by infiltration of fertilizers or other contaminants (Lapworth et al., 2022). Monitoring of the water quality is essential to ensure a water supply that meets the highest standards (Banna et al., 2014). In addition, groundwater pumping might induce the upward migration of saline deep fluids enriched with heavy metals. Fractured basins located over the major tectonic lines occur where the earth's crust was weakened by the numerous tectonic deformations that occurred over geological times. For the same reasons, additional regional investigations near hot or mineralized springs require special precautions.

4.2. Regional Implications

Field investigations and numerical results confirm that bedrock masses with low hydraulic conductivity have exploitable fractured aquifers present along the damage zones associated with tectonic fault zones. The identification of additional sites characterized by important damage zones in contact with weathered blanket aquifers is compelling for development in the rural areas of southeast China. In the bedrock units, a correlation between calibrated hydraulic conductivity and geologic units is not evident due to their low permeability. The YGU and the CGU have the same lithology but their response under the tectonic forces is different due to a different spatial concentration of the damage zones caused by different geological histories. The identification of sites with a high density of damage zones is not possible from field surveys as bedrock and damage zone outcrops are hidden beneath the weathered blanket and dense vegetation. However, at the Longquan site, the damaged zones in the bedrock are associated with a strong morphological contrast (Figure 4a).

The reconstructed damage zones in the bedrock have marked morphological differences from the surrounding bedrock mountains characterized by little fracturing. As the fracturing density increases, the drainage network and the morphology radically change. In areas with fault damage zones, the tributary stream valleys are wide, with a flat bottom surrounded by rounded hills with gentle slopes encompassing the lower sector of the studied area (Figure S4 in Supporting Information S1). On the contrary, mountain slopes of VU (aquitard) are steep with narrow and engraved valleys with an angular to parallel drainage pattern, indicating a competent bedrock less prone to erosion and weathering. In areas with fractured bedrock infiltration is greater which decreases the runoff giving origin to larger valleys with flat floors and a subdendritic drainage pattern. The increased groundwater circulation in these zones has accelerated the erosion processes, contributing to the morphological differences between the low hydraulic conductivity bedrock of the mountain (VU and YGU) and the basin (BU and CGU).

The link between bedrock storage capacity and morphological features is inferred at the regional scale. As the climate conditions over southeastern China can be considered homogeneous (He et al., 2020), the interpretation of the morphological factors throughout the bedrock outcrops is useful for identification of new sites for groundwater exploitation with favorable concentrations of damage zones.

Manual interpretation of satellite images has been demonstrated to be particularly useful for identifying areas with an increased fracture density (Kuehn et al., 2000; Socha, 1983). By observing the spatial contrast of color, tone, and pattern (Allum, 1966; Greenwod, 1969) together with the overlays of DEM and hydrogeological maps at a scale of 1:200,000 (Chinese Geological Surveys, www.cgs.gov.cn), regional information about fracturing was inferred. Within the bedrock outcrops, areas with a change in drainage pattern from parallel and angular to subdendritic (Gupta, 2003) is associated to a morphological transition from mountainous to hilly. These areas were selected as evidence of an accelerated weathering process as well as the presence of thicker laterite soils (WBU). As climatic and lithological conditions are homogeneous throughout southeastern China, these sharp morphological variations are correlated with the local fracturing. Based on the evidence of the Longquan site and the interpretation of the satellite images, 140 sites in southeastern China with fractured bedrock are inferred (Figure 5). Among these 140 identified sites (Figure 5), the sites of Huizhou and Meizhou (Figure S4 in Supporting Information S1) are already exploited by mineral water companies confirming the relationship between morphology and bedrock fracturing.

Hydrological parameters from the Longquan sites can be used to assess preliminary estimation of the groundwater resources. However, the method based on satellite images is qualitative and areas with an incremented fracturing do not necessarily correspond to a homogeneous productive aquifer. Preliminary geoelectrical investigations are necessary to delineate the extension of the damage zones and fine tune the location for water well excavations.

5. Conclusions

To meet their water demand, rural villages in southeastern China primarily rely on surface-water resources, which are limited by rainfall variability and the level of investment in water infrastructure. Identifying productive aquifers is therefore strategic for developing rural areas characterized by low-permeability bedrock. Tectonic fault zones create bedrock damage zones that disaggregate the rock, leading to a distinctive hilly morphology

Figure 5. Satellite image of coastal southeastern China. The pink circles indicate sites where the presence of fractured bedrock is likely due to the morphological, lithological, and climatic similarities with Longquan site. Longquan, Huizhou, and Meizhou sites where mineral water exploitation is already active are marked using cyan circles.

interspersed with flat-floored stream valleys. This setting promotes greater infiltration and groundwater flow while reducing surface runoff.

Despite the relatively modest yield of these fault-related damage zones, the overlying shallow aquifer mitigates excessive drawdown during groundwater pumping by limiting the spread of the cones of depression. Numerical simulations of drought scenarios at the Longquan study site demonstrate that infiltration from the weathered blanket aquifer alleviates stress on the deeper bedrock aquifer.

Based on morphological evidence, 140 sites with similar groundwater potential have been identified throughout southeastern China. The hydrological parameters derived from Longquan offer a useful starting point for estimating the groundwater resources at these sites. Future geoelectrical surveys can help verify the presence of damage zones and guide well-drilling strategies. Ultimately, tapping into these groundwater resources can improve water security, raise living standards, and narrow the economic gap between rural communities and China's rapidly developing coastal regions.

Data Availability Statement

The data set described here is available for download at https://doi.org/10.5281/zenodo.14645296.

Acknowledgments

This work was supported by the National Key R&D program of China (2023YFE0117000), Guangdong Provincial Key Laboratory of Soil and Groundwater Pollution Control (No. 2023B1212060002), and High-level University Special Fund (G030290001). The Authors are grateful to the Zhejiang Engineering Survey and Design Institute Group Co., Ltd and the Bureau of Ecology and Environment of Lishui City at Longquan for the logistic and technical support on the field.

References

Allum, J. A. E. (1966). *Photogeology and regional mapping*. Pergamon Press.108

Banna, M. H., Imran, S., Francisque, A., Najjaran, H., Sadiq, R., Rodriguez, M., & Hoorfar, M. (2014). Online drinking water quality monitoring: Review on available and emerging technologies. *Critical Reviews in Environmental Science and Technology*, *44*(12), 1370–1421. https://doi.org/10.1080/10643389.2013.781936

Bense, V. F., Gleeson, T., Loveless, S. E., Bour, O., & Scibek, J. (2013). Fault zone hydrogeology. *Earth-Science Reviews*, *127*, 171–192. https://doi.org/10.1016/j.earscirev.2013.09.008

Brandt, S. A. (2000). Classification of geomorphological effects downstream of dams. *Catena*, *40*(4), 375–401. https://doi.org/10.1016/S0341-8162(00)00093-X

Caine, J. S., Evans, J. P., & Forster, C. B. (1996). Fault zone architecture and permeability structure. *Geology*, *24*(11), 1025–1028. https://doi.org/10.1130/00917613(1996)024<1025:FZAAPS>2.3.CO;2

Campbell, S. D. G., & Sewell, R. J. (1997). Structural control and tectonic setting of mesozoic volcanism in Hong Kong. *Journal of the Geological Society*, *154*(6), 1039–1052. https://doi.org/10.1144/gsjgs.154.6.1039

Cheng, S., Ye, Z., Li, X., Manga, M., Dorea, C., Chen, Z., et al. (2024). Constructing a toilet standard system for the toilet revolution in China. *Journal of Water, Sanitation and Hygiene for Development*, *14*(4), 291–301. https://doi.org/10.2166/washdev.2024.083

Doherty, J. (2021). *PEST, model independent parameter estimation-user manual, Part I* (7th ed., p. 369). Watermark Numerical Computing.

Famiglietti, J. S. (2014). The global groundwater crisis. *Nature Climate Change*, *4*(11), 945–948. https://doi.org/10.1038/nclimate2425

Freeze, R. A., & Cherry, J. A. (1979). *Groundwater*. Prentice-Hall.

Fu, T., Qi, C., Wang, Z., Li, C., Liu, W., Fu, Y., et al. (2022). Hydrochemical characteristics and quality assessment of groundwater under the impact of seawater intrusion and anthropogenic activity in the coastal areas of Zhejiang and Fujian Provinces, China. *Lithosphere*, *9*(Special 9), 11394857. https://doi.org/10.2113/2022/1394857

Greenwod, J. G. W. (1969). Role of satellite photographs in photogeology. *Nature*, *224*(5218), 506–508. https://doi.org/10.1038/224506b0

Gupta, R. P. (2003). *Remote sensing geology* (p. 655). Springer-Verlag Berlin Heidelberg.

Harbaugh, A. W. (2005). MODFLOW-2005, the U.S. Geological Survey modular groundwater model-the groundwater flow process. In *Chapter 16 of book 6: Modeling techniques, techniques and methods 6-A16* (p. 253). USGS.

He, J., Yang, K., Tang, W., Lu, H., Qin, J., Chen, Y., & Li, X. (2020). The first high-resolution meteorological forcing dataset for land process studies over China. *Scientific Reports*, *7*(1), 25. https://doi.org/10.1038/s41597-020-0369-y

Jasechko, S., Seybold, H., Perrone, D., Fan, Y., Shamsudduha, M., Taylor, R. G., et al. (2024). Rapid groundwater decline and some cases of recovery in aquifers globally. *Nature*, *625*(7996), 715–721. https://doi.org/10.1038/s41586-023-06879-8

Kuang, X., Liu, J., Scanlon, B. R., Jiao, J. J., Jasechko, S., Lancia, M., et al. (2024). The changing nature of groundwater in the global water cycle. *Science*, *383*(6686), eadf0630. https://doi.org/10.1126/science.adf0630

Kuehn, F., King, T. V. V., Hoerig, B., & Peters, D. C. (2000). *Remote sensing for site characterization* (p. 211). Springer-Verlag.

Lachassagne, P., Dewandel, B., & Wyns, R. (2014). The conceptual model of weathered hard rock aquifers and its practical applications. In J. Sharp (Ed.), *Fractured rock hydrogeology*, *Iah - selected papers on hydrogeology* (pp. 13–45). CRC Press. 20142152. https://doi.org/10.1201/b17016-3

Lancia, M., Su, H., Tian, Y., Xu, J., Andrews, C., Lerner, D. N., & Zheng, C. (2020). Hydrogeology of the pearl river Delta, southern China. *Journal of Maps*, *16*(2), 388–395. https://doi.org/10.1080/17445647.2020.1761903

Lancia, M., Yao, Y., Andrews, C., Wang, X., Kuang, X., Ni, J., et al. (2022). The China groundwater crisis: A mechanistic analysis with implications for global sustainability. *Sustainable Horizons*, *4*, 100042. https://doi.org/10.1016/j.horiz.2022.100042

Lapworth, D. J., Boving, T. B., Kreamer, D. K., Kebede, S., & Smedley, P. L. (2022). Groundwater quality: Global threats, opportunities and realising the potential of groundwater. *Science of the Total Environment*, *811*, 152471. https://doi.org/10.1016/j.scitotenv.2021.152471

Lehner, B., Liermann, C. R., Revenga, C., Vörösmarty, C., Fekete, B., Crouzet, P., et al. (2011). High-resolution mapping of the world's reservoirs and dams for sustainable river-flow management. *Frontiers in Ecology and the Environment*, *9*(9), 494–502. https://doi.org/10.1890/100125

Li, J., Ma, Z., Zhang, Y., Dong, S., Li, Y., Lu, M., & Tan, J. (2014). Tectonic evolution of cretaceous extensional basins in Zhejiang Province, eastern South China: Structural and geochronological constraints. *International Geology Review*, *56*(13), 1602–1629. https://doi.org/10.1080/00206814.2014.951978

Liu, X., Xu, Y., Cheng, W., Shen, S., & Horpibulsuk, S. (2017). Investigation of hydraulic parameters of a weathered mylonite fault from field pumping tests: A case study. *Bulletin of Engineering Geology and the Environment*, *76*(4), 1431–1448. https://doi.org/10.1007/s10064-016-0910-6

Long, D., Yang, W., Scanlon, B. R., Zhao, J., Liu, D., Burek, P., et al. (2020). South-to-North Water diversion stabilizing Beijing's groundwater levels. *Nature Communications*, *11*(1), 3665. https://doi.org/10.1038/s41467-020-17428-6

Medici, G., Ling, F., & Shang, J. (2023). Review of discrete fracture network characterization for geothermal energy extraction. *Frontiers in Earth Science*, *11*, 11–2023. https://doi.org/10.3389/feart.2023.1328397

Niswonger, R. G., Panday, S., & Ibaraki, M. (2011). *MODFLOW-NWT, A Newton formulation for MODFLOW-2005* (Vol. 6-A37). U.S. Geological Survey Techniques and Methods.

Rodell, M., Famiglietti, J. S., Wiese, D. N., Reager, J. T., Beaudoing, H. K., Landerer, F. W., & Lo, M. H. (2018). Emerging trends in global freshwater availability. *Nature*, *557*(7707), 651–659. https://doi.org/10.1038/s41586-018-0123-1

Scibek, J. (2020). Multidisciplinary database of permeability of fault zones and surrounding protolith rocks at world-wide sites. *Scientific Data*, *7*(1), 95. https://doi.org/10.1038/s41597-020-0435-5

Shen, D. (2021). *Water resources management of the People`s Republic of China*. Springer Nature. https://doi.org/10.1007/978-3-030-61931-2

Socha, J. (1983). *Fracture-trace analysis for water-well site locations in Precambrian igneous and metamorphic rock in Central Wisconsin*. Miscellaneous Paper 83-5. University of Wisconsin (ed.), (pp. 46), Retrieved from https://wgnhs.wisc.edu/pubshare/MP83-5.pdf [last access on 19 December 2024]

Tigrek, S., & Aras, T. (2011). *Reservoir sediment management*. CRC Press. https://doi.org/10.1201/b11615

United Nations. (2023). The sustainable development goals report – Special edition. Retrieved from https://unstats.un.org/sdgs/report/2023/The-Sustainable-Development-Goals-Report-2023.pdf

Wan, T. (2010). *The tectonics of China: Data, maps and evolution*. Springer.

White, R. (2001). Evacuation of sediments from reservoirs. In *ICE virtual library*. Emerald Publishing. https://doi.org/10.1680/eosfr.29538

Wu, X., Wang, H., Saito, Y., Syvitski, J., Bi, N., Yang, Z., et al. (2022). Boosting riverine sediment by artificial flood in the yellow river and the implication for delta restoration. *Marine Geology*, *448*, 106816. https://doi.org/10.1016/j.margeo.2022.106816

Yao, Y., & Jiang, L. (2021). Urbanization forces driving rural urban income disparity: Evidence from metropolitan areas in China. *Journal of Cleaner Production*, *312*, 127748. https://doi.org/10.1016/j.jclepro.2021.127748

Zhang, K. H. (Ed.) (2006). *China as the world factory*. Routledge. https://doi.org/10.4324/9780203799529

Zheng, C., Liu, J., Cao, G., Kendy, E., Wang, H., & Jia, Y. (2010). Can China cope with its water crisis? - perspectives from the north China plain. *Groundwater Series*, *48*(3), 350–354. https://doi.org/10.1111/j.1745-6584.2010.00695_3.x